

# 1 Prediction, scanning and designing of TNF- $\alpha$ inducing 2 epitopes for human and mouse

3 Anjali Dhall<sup>#</sup>, Sumeet Patiyal<sup>#</sup>, Shubham Choudhury, Shipra Jain, Kashish Narang, Gajendra P. S. Raghava<sup>\*</sup>

4 Department of Computational Biology, Indraprastha Institute of Information Technology, Okhla Phase 3, New  
5 Delhi-110020, India.

6

## 7 Mailing Address of Authors

8 Anjali Dhall (AD): [anjaliid@iiitd.ac.in](mailto:anjaliid@iiitd.ac.in) ORCID ID: <https://orcid.org/0000-0002-0400-2084>

9 Sumeet Patiyal (SP): [sumeetp@iiitd.ac.in](mailto:sumeetp@iiitd.ac.in) ORCID ID: <https://orcid.org/0000-0003-1358-292X>

10 Shubham Choudhury (SC): [shubhamc@iiitd.ac.in](mailto:shubhamc@iiitd.ac.in) ORCID ID: <https://orcid.org/0000-0002-4509-4683>

11 Shipra Jain (SJ): [shipra@iiitd.ac.in](mailto:shipra@iiitd.ac.in) ORCID ID: <https://orcid.org/0000-0002-7045-5188>

12 Kashish Narang (KN): [kashish19026@iiitd.ac.in](mailto:kashish19026@iiitd.ac.in) ORCID ID: <https://orcid.org/0000-0002-8988-9090>

13 Gajendra P. S. Raghava (GPSR): [raghava@iiitd.ac.in](mailto:raghava@iiitd.ac.in) ORCID ID: <https://orcid.org/0000-0002-8902-2876>

14 <sup>#</sup> Equal Authors

15 <sup>\*</sup>Corresponding Author

16 Prof. Gajendra P. S. Raghava

17 Head and Professor

18 Department of Computational Biology

19 Indraprastha Institute of Information Technology, Delhi

20 Okhla Industrial Estate, Phase III, (Near Govind Puri Metro Station)

21 New Delhi, India – 110020 Office: A-302 (R&D Block)

22 Phone: 011-26907444

23 Email: [raghava@iiitd.ac.in](mailto:raghava@iiitd.ac.in)

24 Website: <http://webs.iiitd.edu.in/raghava/>

## 25 **Abstract**

26 Tumor Necrosis Factor alpha (TNF- $\alpha$ ) is a pleiotropic pro-inflammatory cytokine that plays a  
27 crucial role in controlling signaling pathways within the immune cells. Recent studies  
28 reported that the higher expression levels of TNF- $\alpha$  is associated with the progression of  
29 several diseases including cancers, cytokine release syndrome in COVID-19 and autoimmune  
30 disorders. Thus, it is the need of the hour to develop immunotherapies or subunit vaccines to  
31 manage TNF- $\alpha$  progression in various disease conditions. In the pilot study, we have  
32 proposed a host-specific in-silico tool for the prediction, designing and scanning of TNF- $\alpha$   
33 inducing epitopes. The prediction models were trained and validated on the experimentally  
34 validated TNF- $\alpha$  inducing/non-inducing for human and mouse hosts. Firstly, we developed  
35 alignment free (machine learning based models using composition of peptides) methods for  
36 predicting TNF- $\alpha$  inducing peptides and achieved maximum AUROC of 0.79 and 0.74 for  
37 human and mouse hosts, respectively. Secondly, alignment based (using BLAST) method has  
38 been used for predicting TNF- $\alpha$  inducing epitopes. Finally, a hybrid method (combination of  
39 alignment free and alignment-based method) has been developed for predicting epitopes. Our  
40 hybrid method achieved maximum AUROC of 0.83 and 0.77 on an independent dataset for  
41 human and mouse hosts, respectively. We have also identified the potential TNF- $\alpha$  inducing  
42 peptides in different proteins of HIV-1, HIV-2, SARS-CoV-2 and human insulin. Best  
43 models developed in this study has been incorporated in a webserver TNFepitope  
44 (<https://webs.iitd.edu.in/raghava/tnfepitope/>), standalone package and GitLab  
45 (<https://gitlab.com/raghavalab/tnfepitope>).

46

## 47 **Keywords**

48 TNF- $\alpha$  inducing epitopes, Prediction, Designing, Hybrid method, Subunit vaccines

49

## 50 **Key Points**

51

- 52 • TNF- $\alpha$  is a multifunctional pleiotropic pro-inflammatory cytokine.
- 53 • Anti-TNF- $\alpha$  therapy used as an effective treatment in several autoimmune disorders.
- 54 • Composition-based features generated using Pfeature for each peptide sequence.
- 55 • Alignment-based and alignment-free models developed.
- 56 • Prediction and scanning of TNF- $\alpha$  inducing regions in antigens.
- 57 • TNFepitope is available as a web-server, standalone package and GitLab.

## 58 **Author's Biography**

59

60 1. Anjali Dhall is currently working as Ph.D. in Computational Biology from  
61 Department of Computational Biology, Indraprastha Institute of Information  
62 Technology, New Delhi, India.

63

64 2. Sumeet Patiyal is currently working as Ph.D. in Computational biology from  
65 Department of Computational Biology, Indraprastha Institute of Information  
66 Technology, New Delhi, India.

67

68 3. Shubham Choudhury is currently working as Ph.D. in Computational Biology from  
69 Department of Computational Biology, Indraprastha Institute of Information  
70 Technology, New Delhi, India.

71

72 4. Shipra Jain is currently working as Ph.D. in Computational Biology from Department  
73 of Computational Biology, Indraprastha Institute of Information Technology, New  
74 Delhi, India.

75

76 5. Kashish Narang is currently working as MTech. (CSE) at Indraprastha Institute of  
77 Information Technology, New Delhi, India.

78

79 6. Gajendra P. S. Raghava is currently working as Professor and Head of Department of  
80 Computational Biology, Indraprastha Institute of Information Technology, New  
81 Delhi, India.

## 82 **Introduction**

83 Tumor Necrosis Factor alpha (TNF- $\alpha$ ), is a classical, pleiotropic pro-inflammatory cytokine  
84 that function by promoting cellular signal activation and trafficking of leukocytes to  
85 inflammatory sites [1]. During acute inflammation, TNF- $\alpha$  cytokine is released by  
86 macrophages/monocytes or via other cell types (e.g., B cells, T cells, mast cells, fibroblasts),  
87 which further regulates haematopoiesis, immune responses, tumor regression and various  
88 infections [2-6]. TNF- $\alpha$  is the first “adipokine” reported in literature to be produced from  
89 adipose tissue [7-9]. It plays a significant role in various biological processes, including  
90 immunomodulation, fever, inflammatory response, inhibition of tumor formation, and  
91 inhibition of virus replication [10]. In its active form TNF- $\alpha$  molecule exists as a homotrimer,  
92 where it binds to homotrimeric TNFRs receptors to induce signaling [11]. Most of the  
93 downstream functions of TNF- $\alpha$  are executed via binding with two distinct receptors: TNFR1  
94 and TNFR2 [11]. Pleiotropic biological effects of TNF- $\alpha$  are based on the interactions  
95 between TNF and its receptors (both circulating and membrane-bound) [3]. Binding of TNF-  
96  $\alpha$  to its receptor can initiate several signaling pathways, including the activation of  
97 transcription factors (e.g., nuclear factor- $\kappa$ B [NF- $\kappa$ B]), protein kinases (e.g., c-Jun N-  
98 terminal kinase [JNK], p38 MAP kinase), and proteases (e.g., caspases) that markedly impact  
99 immune and inflammatory responses [12].

100

101 Recent studies revealed that TNF- $\alpha$  is involved in various physiological effects such as  
102 induction of pro-inflammatory interleukins (IL-1 and IL-6) [13-15]. Studies also shows that  
103 TNF- $\alpha$  and IL-1 $\beta$  have been found to be implicated in the pathogenesis of myocardial  
104 dysfunction in ischemia-reperfusion injury, sepsis, chronic heart failure, viral myocarditis,  
105 and cardiac allograft rejection [16-18]. In addition, TNF- $\alpha$  also interacts with various  
106 cytokines/chemokines and regulates signaling pathways in various other disease states [19].  
107 For example, Guo et. al., reported that cytokine release syndrome in COVID-19 patients is  
108 associated with the increased levels of TNF- $\alpha$ , IL-6, IL-2, IL-7, and IL-10 cytokines [20]. In  
109 addition, a number of studies reported the direct relationship of TNF- $\alpha$  and IL-6 cytokines in  
110 the severity and survival of COVID-19 patients [21-23]. Therefore, several anti-TNF  
111 inhibitors are available in the market which can block the over production of TNF- $\alpha$  in  
112 different disease conditions. In literature, studies have reported wide use of anti-TNF therapy  
113 for effective treatment of rheumatoid arthritis (RA), spondyloarthropathy, psoriasis and  
114 inflammatory bowel disease [24-27]. In the recent times, anti-TNF- $\alpha$  therapy has reported

115 beneficial effects by not only restoring aberrant TNF-mediated immune mechanisms, but also  
116 by de-activating pathogenic fibroblast-like mesenchymal cells [28].

117

118 As reported in literature, TNF- $\alpha$  is a key cytokine involved in several diseases and their  
119 increasing severity. Therefore, it can act as a primary target cytokine in disease progression.  
120 This creates a need to develop a computational tool, for predicting TNF- $\alpha$  inducing peptides  
121 using sequence information. In present study, we have come up with an in-silico method to  
122 classify the TNF- $\alpha$  inducing and non-inducing epitopes. We have developed this tool using  
123 experimentally validated TNF- $\alpha$  inducing and non-inducing peptides for human and mouse  
124 hosts. In addition, we have used randomly generated peptides from SwissProt database [29].  
125 We have developed prediction models using various machine learning classifiers and  
126 evaluated performance on the independent dataset.

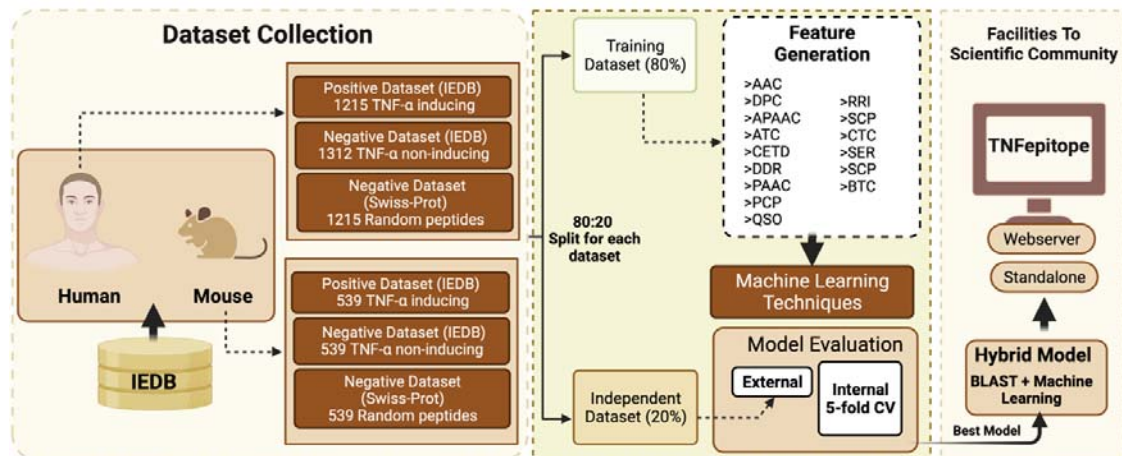
127

## 128 **Material and methods**

### 129 **Overall Workflow**

130 The complete workflow of the current study is illustrated in Figure 1.

131



132

133 **Figure 1: Overall architecture of the study; including data creation, feature generation,**  
134 **model building and webservice**

135

### 136 **Dataset collection and preprocessing**

137 We have collected 3635 TNF- $\alpha$  inducing peptides/epitopes from the immune epitope  
138 database (IEDB [30]). At first, we filtered the dataset based on the hosts and observed that  
139 3177 peptides are experimentally validated on human or mouse hosts, and only a few

140 epitopes are available for other hosts. So, we selected only two major hosts (i.e., human and  
141 mouse). We have checked the length distribution of epitopes and observed that most of the  
142 peptides belong to the range of 8-20 amino-acid residues. After removing the redundancy, we  
143 obtained 1215 and 539 TNF- $\alpha$  inducing epitopes for humans and mouse, respectively.

144 In this study, we have two separate negative datasets for both human and mouse. The first  
145 negative dataset was collected from IEDB, containing 2383 experimentally validated TNF- $\alpha$   
146 non-inducing epitopes for both the hosts. After preprocessing, we obtain 1312 unique TNF- $\alpha$   
147 non-inducing epitopes with a range of (8-20 amino-acids) in the case of human host. On the  
148 other side, we have 539 unique TNF- $\alpha$  non-inducing epitopes for the mouse with 8-20 amino-  
149 acids residues range. Finally, the main dataset for human incorporates 1215 TNF- $\alpha$  inducing  
150 and 1312 TNF- $\alpha$  non-inducing peptides. On the other side, in case of mouse we obtain a total  
151 of 539 TNF- $\alpha$  inducing and 539 non-inducing peptides in the main dataset. The second  
152 negative dataset was created using the Swiss-Prot database [29]. Here, we have generated  
153 random peptides for human and mouse to construct another negative dataset. Finally, the  
154 alternate dataset for human incorporates 1215 TNF- $\alpha$  inducing and 1215 randomly generated  
155 peptides sing Swiss-Prot database. Similarly, in case of mouse we get a total of 539 TNF- $\alpha$   
156 inducing and 539 randomly generated peptides. After generating the final datasets for human  
157 and mouse hosts; each dataset was divided into training and independent/validation set. Here,  
158 the complete dataset splitted into 80:20 ratio where 80% data was used to train the models  
159 and 20% data was used for the validation purpose.

160

161 **Table 1: Distribution of TNF- $\alpha$  inducing and non-inducing peptides extracted from**  
162 **IEDB and Swiss-Prot database**

	<b>Dataset</b>	<b>TNF-<math>\alpha</math> inducing (Positive Dataset)</b>	<b>TNF-<math>\alpha</math> non-inducing (Negative Dataset)</b>	<b>Total</b>
<b>Human</b>	Main Dataset	1215	1312	2527
	Alternate Dataset	1215	1215	2430
<b>Mouse</b>	Main Dataset	539	539	1078
	Alternate Dataset	539	539	1078

163

164

### 165 **Composition-based analysis**

166 We have used Pfeature [31] to calculate the amino acid composition (AAC) of main and  
167 alternate datasets. Using the compositional analysis, we understand the similarity between the

168 different peptide sequences taken from positive and negative datasets. Using the following  
169 equation 1, we have generated a feature vector of length 20, which specify the percent  
170 composition of 20 amino-acid residues.

171

172

$$AAC_i = \frac{AAR_i}{Total\ number\ of\ residues} \times 100$$

173

174 where  $AAC_i$  and  $AAR_i$  are the percentage composition and number of residues of type  $i$  in a  
175 peptide, respectively.

176

### 177 **WebLogo**

178 We have used WebLogo (<http://weblogo.threepplusone.com>) [32] in order to generate  
179 sequence logos of TNF- $\alpha$  inducing epitopes. Here x-axis represents the amino-acid residues  
180 and y-axis presents the bit-score which shows the importance of particular residue at a given  
181 position. WebLogo takes a fixed length vector of input peptide sequences. In order to create a  
182 fix length vector, we have considered eight amino-acids from the N-terminal and eight-  
183 residues from the C-terminal, as eight is the minimum length of eptides in our dataset and  
184 merged them to generated a fixed length vector of sixteen residues for both human and mouse  
185 TNF- $\alpha$  inducing epitopes.

186

### 187 **Feature generation**

188 In the current study, we have calculated a wide range of features using the sequence  
189 information of peptide sequences. We have used Pfeature [31] standalone package in order to  
190 calculate the composition-based features for our datasets. We have computed a total of 1163  
191 features for each epitope/peptide sequence in both positive and negative datasets. We have  
192 computed twelve different types of descriptors/features such as AAC (Amino acid  
193 composition), DPC (Di-peptide composition), APAAC (Amphiphilic pseudo amino acid  
194 composition), ATC (Atomic composition), CETD (Composition-enhanced transition  
195 distribution), DDR (Distance distribution of residue), PAAC (Pseudo amino acid  
196 composition), PCP (Physico-chemical properties composition), QSO (Quasi-sequence order),  
197 RRI (Residue repeat Information), SPC (Shannon entropy of physico-chemical properties),



198 CTC (Conjoint triad descriptors), etc. In this study, we have developed prediction models  
199 using each feature as well as combining all the features.

200

## 201 **Machine learning and Cross-validation Techniques**

202 In order to develop the prediction models, we have used various machine learning algorithms  
203 such as Random Forest (RF), Decision Tree (DT), Gaussian Naive Bayes (GNB), Logistic  
204 Regression (LR), Support Vector Classifier (SVC), K-Nearest Neighbor (KNN) and Extra  
205 Tree (ET). We have trained the parameters on training dataset and predictions were made on  
206 the independent dataset. Scikit-learn [33] python library was used in the study for the  
207 implementation of various classifiers. We have employed five-fold cross validation technique  
208 in order to evade the curse of biasness and overfitting. In the five-fold cross-validation, first  
209 the training dataset was divided into five equal sets; where four sets were used for training  
210 and fifth set was used for testing. This process is repeated five times where each part gets  
211 utilized for testing of the model as shown in some previous studies [34-40]. Of note, the final  
212 performance is the mean of the performance resulted after each iteration.

213

## 214 **Similarity Search Method**

215 We have used BLAST [41] to implement similarity search or alignment-based approach;  
216 where we classify the epitopes as TNF- $\alpha$  inducing and non-inducing on the basis of the  
217 similarity. Here, we have used NCBI-BLAST+ version 2.2.29 (blastp suite) for similarity  
218 search and makeblastdb suite of NCBI-BLAST+ for the creation of custom database. We  
219 have created a custom database using the training dataset; and sequences of validation dataset  
220 were searched against the created database. Based on the hits and their similarity with the  
221 customized database, we assign class as TNF- $\alpha$  inducer or non-inducer. Currently we have  
222 considered only top-hit of BLAST (i.e., if the top-hit of BLAST is against the TNF- $\alpha$  inducer  
223 peptide then the query sequence was assigned as TNF- $\alpha$  inducing peptide or vice-versa). To  
224 identify the optimal value of e-value; we run the BLAST at various e-values cut-offs varying  
225 from  $1e-6$  to  $1e+3$ .

226

## 227 **Hybrid Model**

228 In order to improve the prediction, we have applied the hybrid approach in which we merge  
229 alignment-based (BLAST) and alignment-free (machine learning based prediction). Here,  
230 first we classify the peptide/epitope based on the BLAST. After that, we add '+0.5' score for



231 the correct positive prediction i.e., TNF- $\alpha$  inducing peptide, ‘-0.5’ score integrated for the  
232 negative predictions i.e., TNF- $\alpha$  non-inducing peptide and ‘0’ score if no-hit was found.  
233 Further, we incorporate the prediction score calculated using machine learning based models.  
234 Finally, we combine the BLAST score and machine learning prediction score to make final  
235 predictions.

236

## 237 **Performance Evaluation**

238 The performance of different models were evaluated using standard performance evaluation  
239 parameters sensitivity, specificity, accuracy, Area Under Receiver Operating Characteristics  
240 (AUROC) curve, Area Under the Precision-Recall Curve (AUPRC), Matthews Correlation  
241 Coefficient (MCC), and F1-score. We have computed both threshold-dependent (including  
242 sensitivity, specificity, accuracy, F1-score, and MCC) and independent parameters such as  
243 AUROC and AUPRC. The equations of evaluation parameters is provided in equations (2-6).  
244

$$245 \text{ Sensitivity} = \frac{T_P}{T_P + F_N} \quad [2]$$

$$246 \text{ Specificity} = \frac{T_N}{T_N + F_P} \quad [3]$$

$$247 \text{ Accuracy} = \frac{T_P + T_N}{T_P + T_N + F_P + F_N} \quad [4]$$

$$248 \text{ F1 - Score} = \frac{2T_P}{2T_P + F_P + F_N} \quad [5]$$

$$249 \text{ MCC} = \frac{(T_P * T_N) - (F_P * F_N)}{\sqrt{(T_P + F_P)(T_P + F_N)(T_N + F_P)(T_N + F_N)}} \quad [6]$$

245

246 Where, FP is false positive, FN is false negative, TP is true positive and TN is true negative.

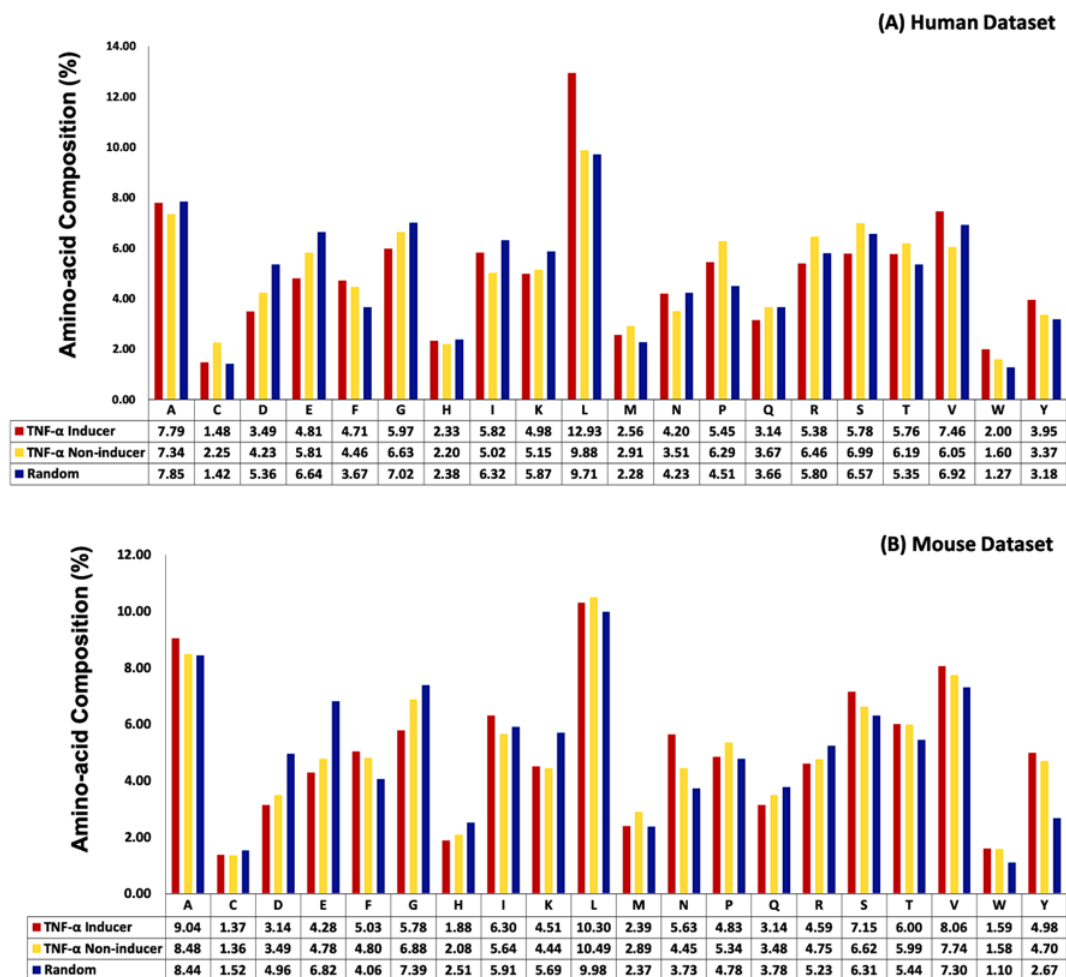
247

## 248 **Results**

### 249 **Compositional Analysis**

250 We have computed amino acid composition for the main and alternate datasets for human  
251 and mouse hosts. After that, we have calculated the average compositions of TNF- $\alpha$  inducing  
252 and non-inducing peptides. As depicted in Figure 2A, in case of human dataset amino acids  
253 such as leucine (L), valine (V), tyrosine (Y), and tryptophan (W) having higher composition  
254 in the TNF- $\alpha$  inducing peptides in comparison with the TNF- $\alpha$  non-inducing and random  
255 peptides. Similarly, the average composition of residues like alanine (A), isoleucine (I),

256 asparagine (N), and serine (S) are more abundant in TNF- $\alpha$  inducing peptides of mouse  
 257 dataset (See Figure 2B).



258  
 259 **Figure 2: Average amino-acid composition of TNF- $\alpha$  inducing, TNF- $\alpha$  non-inducing and**  
 260 **random peptides**

261

## 262 Positional Conservation Analysis

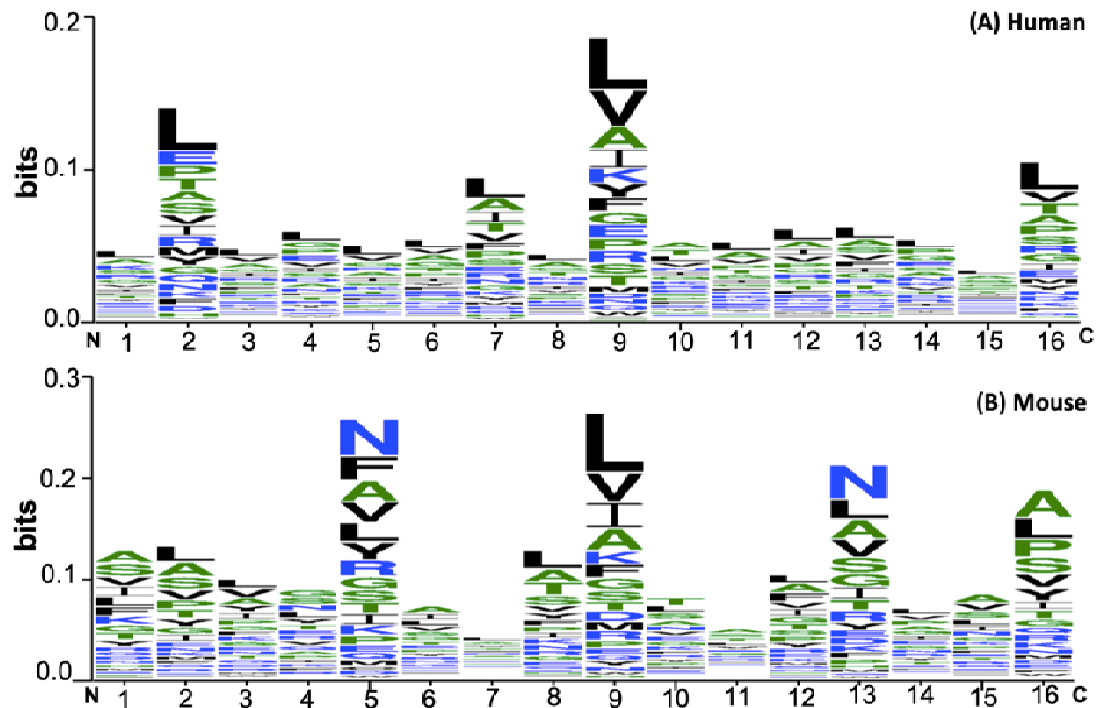
263 In this analysis, we study the preference of residues at particular position in the TNF- $\alpha$   
 264 inducing epitopes for human and mouse dataset. In the case of human TNF- $\alpha$  inducing  
 265 epitopes, residues 'L' is highly conserved at most of the positions, whereas 'V' is preferred at  
 266 9<sup>th</sup> and 16<sup>th</sup> positions; 'A' is located on 7<sup>th</sup>, 9<sup>th</sup>, 10<sup>th</sup>, 11<sup>th</sup>, 12<sup>th</sup>, 13<sup>th</sup> and 16<sup>th</sup> positions (See  
 267 Figure 3A). In the case of mouse, TNF- $\alpha$  inducing epitopes 'L' is highly dominated on 2<sup>nd</sup>,  
 268 3<sup>rd</sup>, 8<sup>th</sup>, 9<sup>th</sup>, 12<sup>th</sup>, 13<sup>th</sup> and 16<sup>th</sup> positions; similarly residue 'N' is highly conserved at 5<sup>th</sup> and

269 13<sup>th</sup> positions; however, 'A' is predominated on 5<sup>th</sup>, 8<sup>th</sup>, 9<sup>th</sup>, 13<sup>th</sup>, 16<sup>th</sup> positions, as shown in  
270 Figure 3B.

271

272

273



274

275

**Figure 3: WebLogo representation of TNF- $\alpha$  inducing peptides in human and mouse**

276

**datasets**

277

## 278 **Machine Learning based Predictions**

279 We have developed prediction models using different classifiers such as DT, RF, GNB,  
280 KNN, SVC, LR and ET on main and alternate datasets of both human and mouse hosts. For  
281 this we have generated 15 different types of composition based features using Pfeature  
282 standalone. We evaluated the performance on different features as well as combining all the  
283 features.

284

## 285 **Performance of Composition-based Features**

286

287 Here, we have computed performance on 15 different features. We have observed that RF  
288 and ET classifiers performed best among the other classifiers (See Supplementary Table S1).

289 As shown in Table 2, in the case of human host, we achieved maximum performance on main

290 dataset with an AUROC of 0.79, MCC of 0.45 on the independent dataset using DPC based  
 291 features. APAAC and SER based features also performed quite well on independent dataset  
 292 with an AUROC of 0.78 and AUPRC of 0.75. In the case of alternate dataset we attains  
 293 maximum AUROC of 0.71, AUPRC of 0.73 and MCC of 0.31 using DPC based features.  
 294 While combining all the features we are getting (0.77 and 0.71) AUROC on main and  
 295 alternate dataset, respectively. Other composition-based features, perform poor on both main  
 296 and alternate dataset. The complete results of all the classifiers for the features are shown in  
 297 Supplementary Table S2.

298

299 **Table 2: Performance of independent dataset developed using 15 types of composition-**  
 300 **based features for human main and alternate datasets**

301

Feature Type	Main Dataset						Alternate Dataset					
	Sens	Spec	Acc	AUROC	AUPRC	MCC	Sens	Spec	Acc	AUROC	AUPRC	MCC
AAC	55.97	58.56	57.31	0.63	0.61	0.15	63.37	66.26	64.82	0.70	0.72	0.30
DPC	72.02	72.62	72.33	0.79	0.76	0.45	68.72	61.73	65.23	0.71	0.73	0.31
ATC	55.97	58.56	57.31	0.63	0.61	0.15	59.67	58.03	58.85	0.61	0.62	0.18
APAAC	68.31	74.91	71.74	0.78	0.75	0.43	63.37	67.49	65.43	0.70	0.73	0.31
BTC	69.55	68.82	69.17	0.69	0.64	0.38	55.97	50.62	53.29	0.55	0.53	0.07
CETD	66.67	70.34	68.58	0.74	0.72	0.37	61.32	61.32	61.32	0.64	0.64	0.23
CTD	61.32	66.92	64.23	0.70	0.65	0.28	62.14	61.73	61.93	0.66	0.68	0.24
DDR	72.02	73.76	72.93	0.77	0.74	0.46	62.55	64.61	63.58	0.70	0.71	0.27
PAAC	68.31	74.14	71.34	0.78	0.75	0.43	65.02	65.43	65.23	0.70	0.72	0.31
PCP	64.61	67.68	66.21	0.73	0.72	0.32	62.96	63.37	63.17	0.67	0.67	0.26
QSO	62.55	71.86	67.39	0.72	0.71	0.35	63.79	65.43	64.61	0.69	0.71	0.29
RRI	62.55	68.06	65.42	0.73	0.70	0.31	62.96	57.20	60.08	0.66	0.69	0.20
SEP	63.37	60.84	62.06	0.69	0.67	0.24	43.62	57.61	50.62	0.51	0.50	0.01
SER	67.08	73.38	70.36	0.78	0.75	0.41	64.61	67.90	66.26	0.70	0.73	0.33
SCP	66.67	73.38	70.16	0.74	0.73	0.40	65.02	62.14	63.58	0.68	0.70	0.27
ALL_COMP	68.31	74.91	71.73	0.77	0.74	0.433	65.43	65.02	65.22	0.71	0.73	0.30

302

303

304

305 In case of mouse dataset, RF-based classifier perform well with an AUROC of 0.74, AUPRC  
 306 of 0.76 and MCC of 0.34 on alternate dataset using DPC as input feature (See Table 3).  
 307 Similarly, we achieved an equivalent performance (i.e., AUROC = 0.72, MCC = 0.30, and  
 308 AUPRC = 0.73) using AAC based features on the alternate dataset. In addition, RRI, DDR  
 309 and APAAC also perform quite well with AUROC>0.72 on alternate dataset. However, the

310 performance of machine learning models is comparatively low on the main dataset. The  
 311 complete results on training and independent dataset is provide in Supplementary Table S3,  
 312 S4.

313 **Table 3: Performance of independent dataset developed using 15 types of composition-**  
 314 **based features for mouse main and alternate datasets**

Feature Type	Main Dataset						Alternate Dataset					
	Sens	Spec	Acc	AUROC	AUPRC	MCC	Sens	Spec	Acc	AUROC	AUPRC	MCC
AAC	62.18	60.56	61.37	0.67	0.66	0.23	64.82	64.82	64.82	0.72	0.73	0.30
DPC	58.47	59.86	59.17	0.63	0.62	0.18	66.67	67.59	67.13	0.74	0.76	0.34
ATC	51.97	50.35	51.16	0.54	0.53	0.02	55.56	62.04	58.80	0.65	0.62	0.18
APAAC	62.18	60.09	61.14	0.65	0.63	0.22	63.89	65.74	64.82	0.72	0.73	0.30
BTC	51.51	52.44	51.97	0.55	0.53	0.04	51.85	58.33	55.09	0.56	0.55	0.10
CETD	56.15	58.24	57.19	0.62	0.63	0.14	63.89	66.67	65.28	0.70	0.73	0.31
CTD	51.51	53.13	52.32	0.56	0.57	0.05	65.74	63.89	64.82	0.68	0.68	0.30
DDR	56.85	59.86	58.35	0.62	0.63	0.17	69.44	67.59	68.52	0.74	0.75	0.37
PAAC	60.79	61.02	60.91	0.65	0.64	0.22	67.59	65.74	66.67	0.72	0.73	0.33
PCP	57.77	61.49	59.63	0.61	0.59	0.19	56.48	69.44	62.96	0.70	0.70	0.26
QSO	58.01	58.47	58.24	0.60	0.59	0.17	61.11	70.37	65.74	0.73	0.74	0.32
RRI	59.86	60.79	60.33	0.63	0.62	0.21	65.74	66.67	66.20	0.75	0.74	0.32
SEP	55.68	54.06	54.87	0.57	0.56	0.10	36.11	51.85	43.98	0.45	0.46	-0.12
SER	60.56	62.41	61.49	0.67	0.66	0.23	67.59	69.44	68.52	0.73	0.74	0.37
SCP	57.77	58.47	58.12	0.61	0.59	0.16	60.19	69.44	64.82	0.69	0.66	0.30
ALL_COMP	62.96	62.96	62.96	0.67	0.67	0.26	64.81	68.51	66.67	0.73	0.73	0.33

315

### 316 **Performance of Hybrid Models**

317

318 In this study, we have developed a hybrid model to classify TNF- $\alpha$  inducing and non-  
 319 inducing

320 peptides. At first, we have used the similarity search approach (BLAST) for the prediction of  
 321 positive and negative peptides. As shown in Table 2 and 3, DPC based features outperformed  
 322 on both human and mouse prediction models. Hence, we combined BLAST similarity scores  
 323 and machine learning scores computed using DPC features to make the final predictions. As  
 324 shown in Supplementary Table S2, RF and ET based models performed well on main and  
 325 alternate human datasets, respectively. We have used DPC features and best models to  
 326 calculate the performance of hybrid models at different e-value cutoffs on independent  
 327 datasets as exhibit in Table 4 for human host. We obtained highest performance at e-value  
 328 (1.00E-01) with AUROC of (0.83 and 0.79), AUPRC of (0.80 and 0.84), MCC of (0.52 and

329 0.41) on main and alternate dataset, respectively (See Table 4). The complete results of  
 330 training and independent datasets are provided in Supplementary Table S3.

331

332 **Table 4: Performance of hybrid model on human main and alternative independent**  
 333 **datasets**

334

E-value	Main Dataset						Alternate Dataset					
	Sens	Spec	Acc	AUROC	AUPRC	MCC	Sens	Spec	Acc	AUROC	AUPRC	MCC
1.00E-06	72.43	76.34	74.46	0.82	0.79	0.49	65.02	65.02	65.02	0.72	0.76	0.30
1.00E-05	73.66	77.48	75.64	0.81	0.77	0.51	67.49	65.84	66.67	0.73	0.77	0.33
1.00E-04	72.84	75.57	74.26	0.81	0.76	0.48	66.26	69.14	67.70	0.73	0.77	0.35
1.00E-03	72.43	77.10	74.85	0.81	0.77	0.50	65.02	69.14	67.08	0.73	0.78	0.34
1.00E-02	74.90	76.72	75.84	0.82	0.77	0.52	68.72	69.55	69.14	0.78	0.83	0.38
1.00E-01	76.13	75.95	76.04	0.83	0.80	0.52	70.37	70.78	70.58	0.79	0.84	0.41
1.00E+00	76.54	75.95	76.24	0.83	0.81	0.53	68.72	67.90	68.31	0.77	0.81	0.37
1.00E+01	73.25	74.81	74.06	0.82	0.79	0.48	67.49	68.31	67.90	0.74	0.78	0.36
1.00E+02	72.84	72.14	72.48	0.82	0.79	0.45	67.08	67.49	67.28	0.73	0.78	0.35

335

336 Besides this, we have applied similar approach on mouse dataset, as provided in  
 337 Supplementary Table S4, RF based model outperforms the other classifier on both main and  
 338 alternate human datasets with DPC based features. Using hybrid model, we achieved highest  
 339 performance at e-value (1.00E-01) with AUROC of (0.70 and 0.77), AUPRC of (0.69 and  
 340 0.81), MCC of (0.28 and 0.34) on main and alternate dataset, respectively. The  
 341 comprehensive results of training and independent datasets are given in Supplementary Table  
 342 S5.

343

344 **Table 5: Performance of hybrid model on mouse main and alternative independent**  
 345 **datasets**

E-value	Main Dataset						Alternate Dataset					
	Sens	Spec	Acc	AUROC	AUPRC	MCC	Sens	Spec	Acc	AUROC	AUPRC	MCC
1.00E-06	61.68	59.81	60.75	0.64	0.61	0.22	65.42	65.42	65.42	0.73	0.74	0.31
1.00E-05	69.16	52.34	60.75	0.63	0.61	0.22	64.49	68.22	66.36	0.73	0.75	0.33
1.00E-04	58.88	59.81	59.35	0.64	0.61	0.19	66.36	66.36	66.36	0.73	0.74	0.33
1.00E-03	62.62	64.49	63.55	0.67	0.65	0.27	66.36	67.29	66.82	0.73	0.74	0.34
1.00E-02	61.68	62.62	62.15	0.68	0.66	0.24	67.29	65.42	66.36	0.75	0.79	0.33
1.00E-01	62.62	65.42	64.02	0.70	0.69	0.28	66.36	67.29	66.82	0.77	0.81	0.34
1.00E+00	61.68	62.62	62.15	0.66	0.64	0.24	68.22	69.16	68.69	0.76	0.78	0.37
1.00E+01	60.75	60.75	60.75	0.66	0.64	0.22	65.42	65.42	65.42	0.71	0.74	0.31

1.00E+02	60.75	60.75	60.75	0.65	0.64	0.22	66.36	65.42	65.89	0.71	0.74	0.32
----------	-------	-------	-------	------	------	------	-------	-------	-------	------	------	------

346

347

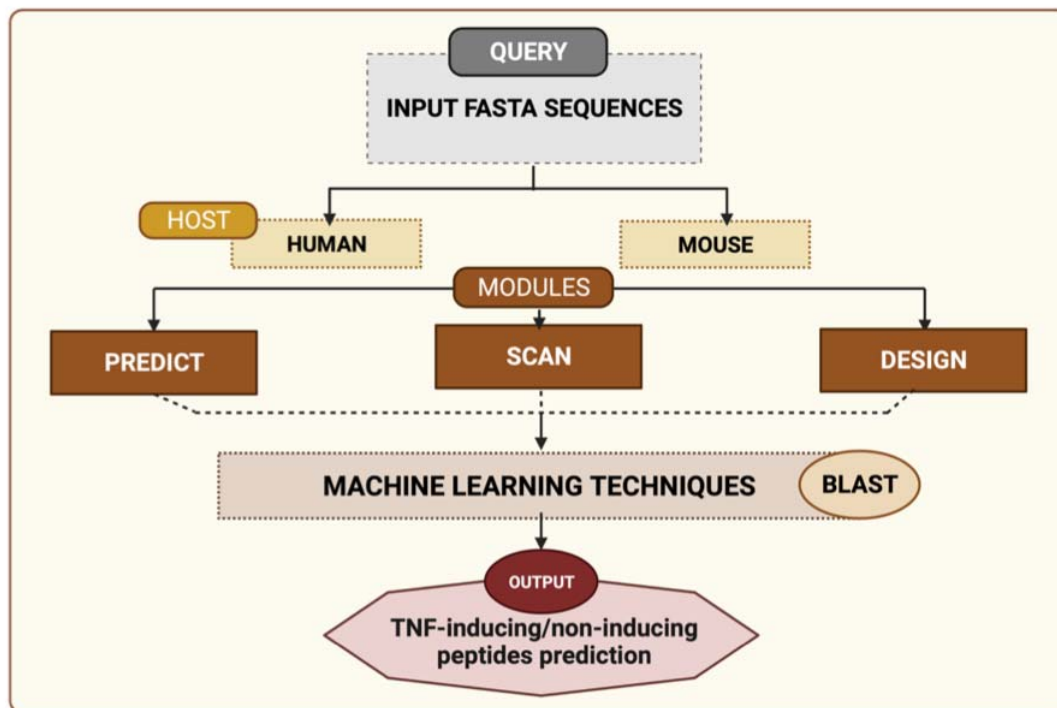
## 348 **Services to Scientific Community**

349

350 We have developed a web-server named ‘TNFepitope’ for the prediction of TNF- $\alpha$  inducing  
351 and non-inducing epitopes using sequence information. The best prediction models for  
352 human and mouse hosts were integrated in the webserver. We have incorporated five major  
353 modules in the server (i) Predict; (ii) Design; (iii) Scan; (iv) Blast Search; and (v) Standalone.  
354 ‘Predict’ module facilitates the users to classify TNF- $\alpha$  inducing peptides from non-inducing  
355 peptides. The ‘Design’ module provide facility to the user to design/create all possible  
356 mutants of query sequence and predict if that can induce the TNF- $\alpha$  release. The ‘Scan’  
357 module allows the user to map/scan the TNF- $\alpha$  secretion portion in the given protein  
358 sequence. The ‘BLAST Search’ module entirely based on similarity search algorithm, the  
359 input sequence is hit against the customized database created using the known TNF- $\alpha$   
360 inducing and non-inducing peptides. The submitted amino-acid sequence is predicted as  
361 TNF- $\alpha$  inducer/non-inducer based on the similarity. ‘TNFepitope’ server was developed  
362 using HTML, JAVA and PHP scripts; it is compatible with a number of devices such as  
363 laptops, iPhone, phones, etc. The webserver (<https://webs.iiitd.edu.in/raghava/tnfepitope>),  
364 standalone package (<https://webs.iiitd.edu.in/raghava/tnfepitope/package.php>) and GitLab  
365 (<https://gitlab.com/raghavalab/tnfepitope>) are freely-accessible. Figure 4 depicts all the major  
366 modules of TNFepitope webserver.

367





368

369

**Figure 4: Schematic representation of different modules of TNFepitope server**

370

### 371 Case Study

372 In order to demonstrate the application of our work, we predicted TNF- $\alpha$  inducing epitopes  
373 using 'Scan' module of TNFepitope webserver with default parameters (i.e., length of peptide  
374 15 and threshold 0.45 with the hybrid method). Here, we have used three viral proteins  
375 (envelope glycoprotein of HIV-1, HIV-2, and surface glycoprotein/spike protein of SARS-  
376 CoV-2), two human proteins (insulin protein and insulin receptor protein) and food protein  
377 (rice Q10MI4). As depicted in Table 6, we does not found any BLAST hits against rice  
378 protein, it means that it does not activate/induce TNF- $\alpha$  production. This strategy can be used  
379 to scan TNF- $\alpha$  inducing regions in other foods or Genetically modified (GM) foods.  
380 Similarly, in the case of human insulin receptor protein, we do not found any hits.  
381 Interestingly, we discovered that human insulin hormone which is a small protein contains  
382 highest percentage of TNF- $\alpha$  inducing regions i.e., 55.21% (See Table 6). Which completely  
383 shows that elevation in insulin levels is responsible for the production of TNF- $\alpha$   
384 peptides/epitopes. This observation agree with the previous studies where they have  
385 demonstrated that insulin resistance patients have higher levels of TNF- $\alpha$  [42, 43].

386 In addition, various studies have reported that elevated levels of TNF- $\alpha$  is associated with the  
387 pathogenesis of viral infections such as (human immunodeficiency virus (HIV) and SARS-

388 CoV-2) [20, 44-46]. As shown in Table 6, the envelope proteins of HIV-1 and HIV-2  
 389 possesses 24.82% and 26.48% TNF- $\alpha$  inducing regions, while the spike protein of SARS-  
 390 CoV-2 have 36.38% TNF- $\alpha$  inducers, which supports the previous studies where severity in  
 391 COVID-19 patients is associated with the high levels of TNF- $\alpha$ . In Supplementary Table S7,  
 392 we have provided the top-most TNF- $\alpha$  inducing epitopes of HIV-1, HIV-2, spike protein and  
 393 human insulin protein. The complete results for each protein in provided in Supplementary  
 394 Table S8-S13. These results indicates that our study can be used to measure the levels of  
 395 TNF- $\alpha$  in different viruses. We hope our findings anticipate the scientific community,  
 396 working in the era of subunit vaccine designing against deadly viruses and other autoimmune  
 397 diseases that can be proliferated by the elevation of TNF- $\alpha$ .

398 **Table 6: Potential TNF- $\alpha$  inducing epitopes predicted by Protein Scan module of**  
 399 **TNFepitope server in 3 viral proteins (HIV-1, HIV-2, and SARS-CoV-2), 2 human**  
 400 **proteins (insulin and insulin receptor) and 1 food protein (rice Q10MI4).**

401

Protein Name	Length	TNF- $\alpha$ inducing epitopes (Score>0.45)		TNF- $\alpha$ inducing epitopes (Score>0.70)		BLAST Hit (Positive)	
		Number of epitopes	Percentage (%)	Number of epitopes	Percentage (%)	Number of epitopes	Percentage (%)
Envelope glycoprotein (HIV-1)	834	207	24.82%	12	1.43%	9	1.08%
Envelope glycoprotein (HIV-2)	846	224	26.48%	7	0.82%	7	0.83%
Spike Protein (SARS-CoV-2)	1259	458	36.38%	251	19.94%	251	19.94%
Insulin protein (Human)	96	53	55.21%	52	54.16%	26	27.08%
Insulin receptor protein (Human)	1368	211	15.42%	0	0.00%	0	0.00%
Food (Rice protein Q10MI4)	881	167	18.96%	0	0.00%	0	0.00%

402

403

## 404 Discussion and Conclusion

405 Major histocompatibility complex region encodes numbers of proteins including human  
 406 leukocyte antigen (HLAs) which are necessary for self-recognition, cytokine genes like TNF,  
 407 LTA, LTB which are responsible for the inflammations [47]. TNF- $\alpha$  is an important  
 408 inflammatory cytokine released by T cells or macrophages and control a number of signalling  
 409 pathways within the immune cells; leads to necrosis or cell death [3, 4]. These pathways  
 410 result in a range of biological responses, such as cell proliferation, differentiation, and

411 survival. TNF- $\alpha$  cytokine employed for cancer treatment and perform anti-cancer activities  
412 by inducing inflammation, immune response, and tumor cell apoptosis [48-50]. However,  
413 improper and excessive activation of TNF signalling pathway may results into the emergence  
414 of pathological diseases such as HIV-I, anorexia, cachexia, obesity, autoimmune disorders  
415 including rheumatoid arthritis, diabetes, inflammatory bowel disease, and Crohn's diseases  
416 [51-59]. Several TNF- $\alpha$  inhibitors such as infliximab, etanercept, golimumab, and  
417 certolizumab and adalimumab have been developed and approved for clinical use to cure  
418 diseases which are associated with abnormal/excessive TNF- $\alpha$  secretion [54, 60].

419

420 Mortaz et. al., also report the higher level of soluble TNF- $\alpha$  in the patients of COVID-19 in  
421 comparison with the healthy control [61]. Therefore, it is crucial to check for the existence of  
422 TNF- $\alpha$  inducing epitopes or to use anti-TNF therapy in a variety of diseases. In the current  
423 study, we have attempted to understand the nature of TNF- $\alpha$  inducing peptides and built a  
424 prediction model to recognize the epitopes which can induce TNF- $\alpha$  secretion. Dataset play  
425 major role in developing machine learning models, hence we have collected experimentally  
426 validated TNF- $\alpha$  inducing and non-inducing peptides for human and mouse. In case of  
427 alternate negative dataset we have generated random peptides using Swiss-Prot database. To  
428 investigate the composition and positional preference, sequence logo and compositional  
429 analytical analysis were conducted. We found that TNF- $\alpha$  inducing epitopes are rich in the  
430 amino acid residue (L) in human and (N) in mouse datasets. Then after, we employed  
431 'Pfeature' to compute 15 types of compositional features using the standalone package.

432

433 We have used a number of machine-learning classifiers in order to develop prediction  
434 models. Our results indicate that di-peptide composition based features performed best in the  
435 case of main and alternate datasets for both human and mouse models. Using DPC based  
436 features we have achieved highest AUROC of 0.79 and 0.74 on the human and mouse  
437 independent dataset. Of note, our hybrid model (BLAST + machine learning) outperformed  
438 others with an AUROC of 0.83 and 0.77 on the human and mouse independent dataset. We  
439 have used the best models and created a web server 'TNFepitope' for the scientific  
440 community, along with a standalone package. TNFepitope  
441 (<https://webs.iitd.edu.in/raghava/tnfepitope>) is publicly accessible and provide facilities to  
442 predict, design, and scan the TNF- $\alpha$  inducing regions. In addition, we have used the 'Scan'  
443 module of TNFepitope server for the prediction of TNF- $\alpha$  inducing epitopes in the spike  
444 protein of SARS-CoV-2, envelope protein (HIV-1 and HIV-2), insulin protein, insulin

445 protein receptor of human and rice protein. We observed higher percentage of TNF- $\alpha$   
446 inducing regions in human insulin protein, followed by spike protein of SARS-CoV-2 and  
447 envelope protein (HIV-1 and HIV-2). We believe that this work will be helpful for the  
448 researchers in the development of computer-aided vaccine design and enabling them to create  
449 subunit vaccines that elicit the appropriate immune response against several TNF- $\alpha$   
450 associated diseases.

## 451 **Funding Source**

452 The current work has received grant from the Department of Bio-Technology (DBT), Govt.  
453 of India, India.

## 454 **Conflict of interest**

455 The authors declare no competing financial and non-financial interests.

## 456 **Authors' contributions**

457 AD and GPSR collected and processed the datasets. AD, SP, KN and GPSR implemented the  
458 algorithms and developed the prediction models. AD, SP and GPSR analysed the results. SC,  
459 AD and SP created the web server. AD, SJ, SP and SC and GPSR penned the manuscript.  
460 GPSR conceived and coordinated the project. All authors have read and approved the final  
461 manuscript.

## 462 **Acknowledgements**

463 Authors are thankful to the Department of Bio-Technology (DBT) and Department of  
464 Science and Technology (DST-INSPIRE) for fellowships and the financial support and  
465 Department of Computational Biology, IIITD New Delhi for infrastructure and facilities.

## 466 **References**

- 467 1. Sethi JK, Hotamisligil GS. Metabolic Messengers: tumour necrosis factor, *Nat Metab*  
468 2021;3:1302-1312.
- 469 2. Aggarwal BB. Signalling pathways of the TNF superfamily: a double-edged sword,  
470 *Nat Rev Immunol* 2003;3:745-756.
- 471 3. Idriss HT, Naismith JH. TNF alpha and the TNF receptor superfamily: structure-  
472 function relationship(s), *Microsc Res Tech* 2000;50:184-195.

- 473 4. Holbrook J, Lara-Reyna S, Jarosz-Griffiths H et al. Tumour necrosis factor signalling  
474 in health and disease, *F1000Res* 2019;8.
- 475 5. Adams AB, Larsen CP, Pearson TC et al. The role of TNF receptor and TNF  
476 superfamily molecules in organ transplantation, *Am J Transplant* 2002;2:12-18.
- 477 6. Wang B, Song N, Yu T et al. Expression of tumor necrosis factor-alpha-mediated  
478 genes predicts recurrence-free survival in lung cancer, *PLoS One* 2014;9:e115945.
- 479 7. Janowska JD. C1q/TNF-related Protein 1, a Multifunctional Adipokine: An Overview  
480 of Current Data, *Am J Med Sci* 2020;360:222-228.
- 481 8. Wang T, He C. Pro-inflammatory cytokines: The link between obesity and  
482 osteoarthritis, *Cytokine Growth Factor Rev* 2018;44:38-50.
- 483 9. Fantuzzi G. Adipose tissue, adipokines, and inflammation, *J Allergy Clin Immunol*  
484 2005;115:911-919; quiz 920.
- 485 10. You K, Gu H, Yuan Z et al. Tumor Necrosis Factor Alpha Signaling and  
486 Organogenesis, *Front Cell Dev Biol* 2021;9:727075.
- 487 11. Locksley RM, Killeen N, Lenardo MJ. The TNF and TNF receptor superfamilies:  
488 integrating mammalian biology, *Cell* 2001;104:487-501.
- 489 12. Pasparakis M, Vandenabeele P. Necroptosis and its role in inflammation, *Nature*  
490 2015;517:311-320.
- 491 13. Old LJ. Tumor necrosis factor, *Sci Am* 1988;258:59-60, 69-75.
- 492 14. Grivennikov SI, Karin M. Inflammatory cytokines in cancer: tumour necrosis factor  
493 and interleukin 6 take the stage, *Ann Rheum Dis* 2011;70 Suppl 1:i104-108.
- 494 15. Saklatvala J, Davis W, Guesdon F. Interleukin 1 (IL1) and tumour necrosis factor  
495 (TNF) signal transduction, *Philos Trans R Soc Lond B Biol Sci* 1996;351:151-157.
- 496 16. Cain BS, Meldrum DR, Dinarello CA et al. Tumor necrosis factor-alpha and  
497 interleukin-1beta synergistically depress human myocardial function, *Crit Care Med*  
498 1999;27:1309-1318.
- 499 17. Bryant D, Becker L, Richardson J et al. Cardiac failure in transgenic mice with  
500 myocardial expression of tumor necrosis factor-alpha, *Circulation* 1998;97:1375-1381.
- 501 18. Muller-Werdan U, Buerke M, Ebelt H et al. Septic cardiomyopathy - A not yet  
502 discovered cardiomyopathy?, *Exp Clin Cardiol* 2006;11:226-236.
- 503 19. Parameswaran N, Patial S. Tumor necrosis factor-alpha signaling in macrophages,  
504 *Crit Rev Eukaryot Gene Expr* 2010;20:87-103.
- 505 20. Guo Y, Hu K, Li Y et al. Targeting TNF-alpha for COVID-19: Recent Advanced and  
506 Controversies, *Front Public Health* 2022;10:833967.

- 507 21. Halim C, Mirza AF, Sari MI. The Association between TNF-alpha, IL-6, and Vitamin  
508 D Levels and COVID-19 Severity and Mortality: A Systematic Review and Meta-Analysis,  
509 Pathogens 2022;11.
- 510 22. Del Valle DM, Kim-Schulze S, Huang HH et al. An inflammatory cytokine signature  
511 predicts COVID-19 severity and survival, Nat Med 2020;26:1636-1643.
- 512 23. Santa Cruz A, Mendes-Frias A, Oliveira AI et al. Interleukin-6 Is a Biomarker for the  
513 Development of Fatal Severe Acute Respiratory Syndrome Coronavirus 2 Pneumonia, Front  
514 Immunol 2021;12:613422.
- 515 24. Dreyer L, Mellekjær L, Hetland ML. [Cancer in arthritis patients after anti-tumour  
516 necrosis factor therapy], Ugeskr Laeger 2009;171:506-511.
- 517 25. Menegatti S, Bianchi E, Rogge L. Anti-TNF Therapy in Spondyloarthritis and  
518 Related Diseases, Impact on the Immune System and Prediction of Treatment Responses,  
519 Front Immunol 2019;10:382.
- 520 26. Plasencia C, Pascual-Salcedo D, Garcia-Carazo S et al. The immunogenicity to the  
521 first anti-TNF therapy determines the outcome of switching to a second anti-TNF therapy in  
522 spondyloarthritis patients, Arthritis Res Ther 2013;15:R79.
- 523 27. Peyrin-Biroulet L. Anti-TNF therapy in inflammatory bowel diseases: a huge review,  
524 Minerva Gastroenterol Dietol 2010;56:233-243.
- 525 28. Evangelatos G, Bamias G, Kitas GD et al. The second decade of anti-TNF-a therapy  
526 in clinical practice: new lessons and future directions in the COVID-19 era, Rheumatol Int  
527 2022.
- 528 29. Bairoch A, Apweiler R. The SWISS-PROT protein sequence database and its  
529 supplement TrEMBL in 2000, Nucleic Acids Res 2000;28:45-48.
- 530 30. R V, S M, Ja O et al. The Immune Epitope Database (IEDB): 2018 update, Nucleic  
531 acids research 2019;47:D339-D343.
- 532 31. Pande A, Patiyal S, Lathwal A et al. Computing wide range of protein/peptide  
533 features from their sequence and structure, BioRxiv 2019:599126-599126.
- 534 32. Crooks GE, Hon G, Chandonia JM et al. WebLogo: a sequence logo generator,  
535 Genome Res 2004;14:1188-1190.
- 536 33. Pedregosa F, Varoquaux G, Gramfort A et al. Scikit-learn: Machine learning in  
537 Python, the Journal of machine Learning research 2011;12:2825-2830.
- 538 34. Dhall A, Patiyal S, Sharma N et al. Computer-aided prediction and design of IL-6  
539 inducing peptides: IL-6 plays a crucial role in COVID-19, Brief Bioinform 2021;22:936-945.

- 540 35. Dhall A, Patiyal S, Raghava GPS. HLAnPred: a method for predicting promiscuous  
541 non-classical HLA binding sites, *Brief Bioinform* 2022.
- 542 36. Dhall A, Patiyal S, Sharma N et al. Computer-aided prediction of inhibitors against  
543 STAT3 for managing COVID-19 associate cytokine storm 2021.
- 544 37. Sharma N, Patiyal S, Dhall A et al. AlgPred 2.0: an improved method for predicting  
545 allergenic proteins and mapping of IgE epitopes, *Brief Bioinform* 2020.
- 546 38. Kumar V, Patiyal S, Dhall A et al. B3Pred: A Random-Forest-Based Method for  
547 Predicting and Designing Blood-Brain Barrier Penetrating Peptides, *Pharmaceutics* 2021;13.
- 548 39. Sumeet Patiyal AD, Gajendra P. S. Raghava\*. DBpred: A deep learning method for  
549 the prediction of DNA  
550 interacting residues in protein sequences, *BioRxiv* 2021.
- 551 40. Patiyal S, Agrawal P, Kumar V et al. NAGbinder: An approach for identifying  
552 N-acetylglucosamine interacting residues of a protein from its primary sequence, *Protein*  
553 *Science* 2020;29:201-210.
- 554 41. McGinnis S, Madden TL. BLAST: at the core of a powerful and diverse set of  
555 sequence analysis tools, *Nucleic Acids Res* 2004;32:W20-25.
- 556 42. Akash MSH, Rehman K, Liaqat A. Tumor Necrosis Factor-Alpha: Role in  
557 Development of Insulin Resistance and Pathogenesis of Type 2 Diabetes Mellitus, *J Cell*  
558 *Biochem* 2018;119:105-110.
- 559 43. Swaroop JJ, Rajarajeswari D, Naidu JN. Association of TNF-alpha with insulin  
560 resistance in type 2 diabetes mellitus, *Indian J Med Res* 2012;135:127-130.
- 561 44. Ablamunits V, Lepsy C. Blocking TNF signaling may save lives in COVID-19  
562 infection, *Mol Biol Rep* 2022;49:2303-2309.
- 563 45. Planes R, Serrero M, Leghmari K et al. HIV-1 Envelope Glycoproteins Induce the  
564 Production of TNF-alpha and IL-10 in Human Monocytes by Activating Calcium Pathway,  
565 *Sci Rep* 2018;8:17215.
- 566 46. Pasquereau S, Kumar A, Herbein G. Targeting TNF and TNF Receptor Pathway in  
567 HIV-1 Infection: from Immune Activation to Viral Reservoirs, *Viruses* 2017;9.
- 568 47. Shiina T, Hosomichi K, Inoko H et al. The HLA genomic loci map: expression,  
569 interaction, diversity and disease, *J Hum Genet* 2009;54:15-39.
- 570 48. Shen J, Xiao Z, Zhao Q et al. Anti-cancer therapy with TNFalpha and IFNgamma: A  
571 comprehensive review, *Cell Prolif* 2018;51:e12441.
- 572 49. Wang X, Lin Y. Tumor necrosis factor and cancer, buddies or foes?, *Acta Pharmacol*  
573 *Sin* 2008;29:1275-1288.



- 574 50. Montfort A, Colacios C, Levade T et al. The TNF Paradox in Cancer Progression and  
575 Immunotherapy, *Front Immunol* 2019;10:1818.
- 576 51. Lane BR, Markovitz DM, Woodford NL et al. TNF-alpha inhibits HIV-1 replication  
577 in peripheral blood monocytes and alveolar macrophages by inducing the production of  
578 RANTES and decreasing C-C chemokine receptor 5 (CCR5) expression, *J Immunol*  
579 1999;163:3653-3661.
- 580 52. Vaughan VC, Martin P, Lewandowski PA. Cancer cachexia: impact, mechanisms and  
581 emerging treatments, *J Cachexia Sarcopenia Muscle* 2013;4:95-109.
- 582 53. Choy EH, Panayi GS. Cytokine pathways and joint inflammation in rheumatoid  
583 arthritis, *N Engl J Med* 2001;344:907-916.
- 584 54. Jang DI, Lee AH, Shin HY et al. The Role of Tumor Necrosis Factor Alpha (TNF-  
585 alpha) in Autoimmune Disease and Current TNF-alpha Inhibitors in Therapeutics, *Int J Mol*  
586 *Sci* 2021;22.
- 587 55. Adegbola SO, Sahnun K, Warusavitarne J et al. Anti-TNF Therapy in Crohn's  
588 Disease, *Int J Mol Sci* 2018;19.
- 589 56. Levin AD, Wildenberg ME, van den Brink GR. Mechanism of Action of Anti-TNF  
590 Therapy in Inflammatory Bowel Disease, *J Crohns Colitis* 2016;10:989-997.
- 591 57. Sands BE, Kaplan GG. The role of TNFalpha in ulcerative colitis, *J Clin Pharmacol*  
592 2007;47:930-941.
- 593 58. Lis K, Kuzawinska O, Balkowiec-Iskra E. Tumor necrosis factor inhibitors - state of  
594 knowledge, *Arch Med Sci* 2014;10:1175-1185.
- 595 59. Raychaudhuri SP, Raychaudhuri SK. Biologics: target-specific treatment of systemic  
596 and cutaneous autoimmune diseases, *Indian J Dermatol* 2009;54:100-109.
- 597 60. Stenvinkel P, Ketteler M, Johnson RJ et al. IL-10, IL-6, and TNF-alpha: central  
598 factors in the altered cytokine network of uremia--the good, the bad, and the ugly, *Kidney Int*  
599 2005;67:1216-1233.
- 600 61. Mortaz E, Tabarsi P, Jamaati H et al. Increased Serum Levels of Soluble TNF-alpha  
601 Receptor Is Associated With ICU Mortality in COVID-19 Patients, *Front Immunol*  
602 2021;12:592727.
- 603